

CAD of an X-Band TWT Interaction Circuit with Experimental Validation

Daniel Teixeira Lopes

Instituto de Pesquisas Energéticas e Nucleares - IPEN
São Paulo, SP, Brazil
danieltl@usp.br

Cláudio Costa Motta

Universidade de São Paulo - USP
São Paulo, SP, Brazil
ccmotta@usp.br

Abstract— In this paper we present results obtained while testing the 3D electromagnetic solver CST Microwave Studio as a CAD tool in the design of some parts of the beam-wave interaction circuit of an X-band traveling-wave tube. A pair of impedance transformers, present in the input and output microwave ports of the interaction circuit, was characterized by simulating and measuring its voltage stand wave ratio. The interaction circuit based on a ring-bar slow-wave structure was simulated using both the eigenmode and the frequency domain solvers of the CST Microwave Studio. The phase velocity and the interaction impedance, also named “cold parameters”, were simulated by direct and indirect methods and the results compared to experimental ones.

Keywords— component; slow-wave structure; impedance transformer; phase velocity; interaction impedance.

I. INTRODUCTION

In many microwave circuits it is often necessary to match different impedance lines to improve the circuit efficiency by minimizing reflections over a desired frequency range. With respect to traveling-wave tubes (TWTs), in virtually all cases the beam-wave interaction circuit and the external waveguide line have different impedance levels. It is indeed necessary to use some matching solution to make a satisfactory transition between both lines minimizing reflections from the microwave ports over the device's bandwidth.

The beam-wave interaction circuit of a TWT is composed by a slow-wave structure (SWS - helices in the most cases) surrounded by a circular section shield guide. The so called “cold parameters” of the interaction circuit are the phase velocity and the interaction impedance. These two quantities are input variables in the determination of the large signal behavior of a TWT. Therefore, accurate prediction and measurement of both quantities are very relevant in the development of efficient devices.

In this paper we present some results obtained from the validation of the commercial 3D electromagnetic solver CST Microwave Studio. This code has been used to aid in the design and in the improvement of an X-band traveling-wave tube. We present here some results of the design of a matching ladder structure for the interaction circuit ports. We also present results from the simulation of the cold test parameters of the

interaction circuit using direct and indirect methods. These results are compared to experimental ones for validation.

II. IMPEDANCE TRANSFORMER SIMULATION

A preliminary impedance transformer, to be used in an X-band TWT, was theoretically synthesized and its dimensions were used in CST Microwave Studio simulations, as input parameter. An illustrative view of the impedance transformer is shown in Figure 1(a). The WR-90 standard used in X-band transmission lines is indicated by the number 10.16 mm in the larger port. The other port dimension matches with the interaction circuit impedance. Another modified impedance transformer, that will compose the new interaction circuit of the TWT under development, was designed and characterized in order to validate the code used. Due to the impossibility of measuring one single impedance transformer section, two sections connected by the smaller port, like the assembly illustrated in Figure 1(b), were also simulated. This result was used for validating the simulation of a single section.

The measurements were performed using one port of a vector network analyzer (VNA) HP N5230A PNA. The voltage stand-wave ratio (VSWR) was measured over 8.0 to 9.5 GHz. After calibration with the X-band calibration kit, a VNA port was connected to one of the transformer ports, while the other transformer port was connected to an X-Band matched load. The comparison between simulated and experimental results

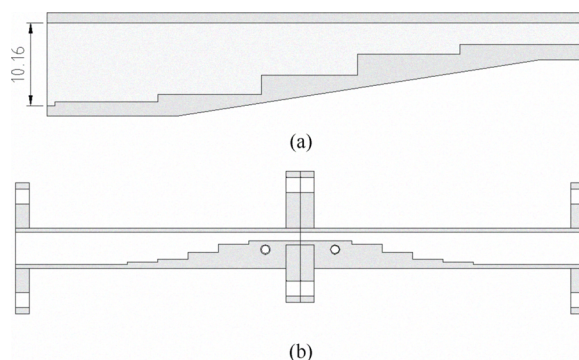


Figure 1 – (a) Illustration of one impedance transformer section from the WR-90 standard, indicated by the 10.16 millimeters dimension, for the interaction circuit line port. (b) Measurement and simulation assembly of a pair of single sections.

This work was supported in part by FAPESP (The State of São Paulo Research Agency) under project 2008/05286-1 and FINEP (Research and Projects Financing) under contract 01.06.0911.01.

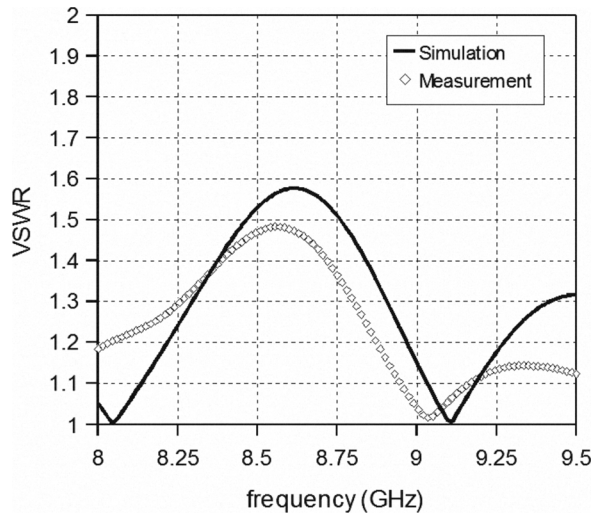


Figure 2 – VSWR as function of frequency for the assembly shown in Figure 1(b) for the preliminary impedance transformers.

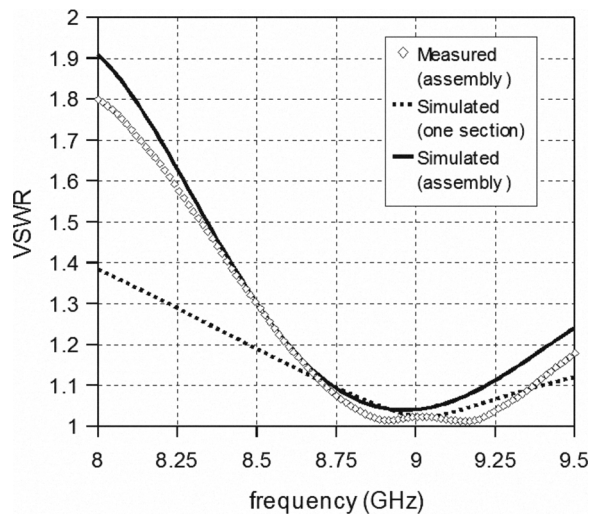


Figure 3 – VSWR as function of frequency for the assembly shown in Figure 1(b) for a pair of improved impedance transformers.

for both the original and the improved transformer is shown in Figures 2 and 3, respectively.

The simulation discrepancy for the preliminary device is about 10-17% at the ends and about 5% in the middle of the presented frequency range. These discrepancies may be attributed to imperfections in the manufacturing of the device, as it was verified. So, the fabricated ladder structure may differ somewhat from that simulated.

Figure 3 shows the comparison between simulation and experimental results for the modified impedance transformer. The simulated curve fits the experimental data better than in the previous case. The discrepancy is about 5% in the ends of the presented frequency band and less than 1% in the middle. By the way, the experimental data indicates a VSWR level

lower than that simulated in the interest region. The dashed line refers to one section transformer, which could not be measured. However, since the code was validated for the assembly case, this result can be considered reliable.

III. THE INTERACTION CIRCUIT

In the TWT under study, the slow-wave structure consists on a ring-bar supported by beryllia shafts. However, the beryllia supports were not included in this paper since this part of the fabrication process is not reached yet. This circuit was analytically studied in other work [1] and analytical results were compared to experimental and simulation ones. Here, we use the 3D eigensolver and the frequency domain solver from CST Microwave Studio software package to make a deeper investigation on the methods for obtaining cold parameters of slow-wave structures.

A. Modelling the Slow-Wave Structure

A modeled slow-wave structure is shown in Figure 4(a), in which one period with periodic boundary conditions in propagation direction was constructed. This model was used together with the eigenmode solver, which varies the phase-shift between periodic boundary conditions and gives the eigenfrequencies related to a number of chosen modes.

Another approach used the frequency domain solver to obtain the phase of the axial electric field as a function of the axial position for a number of frequencies. In this case the modeled structure has to be composed by a minimum number of periodic cells as shown in Figure 4(b) in order to approximate an infinite length structure.

B. Simulation with the eigenmode solver

The normalized phase velocity v_p/c was obtained from the eigensolver configuring the post processing routines to calculate

$$v_p(f)/c = k_0(f)/\beta(f), \quad (1)$$

$$\text{where } k_0(f) = 2\pi f/c, \quad (2)$$

is the free space propagation constant, and

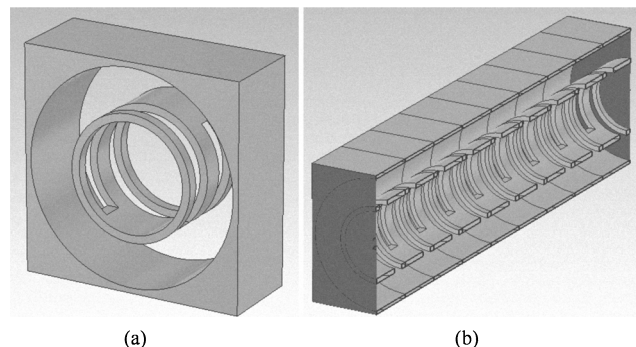


Figure 4 – Slow-wave structure model used with the eigenmode solver (a) and used with the frequency domain solver (b).

$$\beta(f) = \frac{\Delta\Phi(f)}{p} \frac{\pi}{180}, \quad (3)$$

is the axial propagation constant in the slow-wave structure. $\Delta\Phi(f)$ is the phase shift between the periodic boundaries and p is the structure period. The factor $\pi/180$ is used because $\Delta\Phi(f)$ is given in degrees.

The interaction impedance $K_0(f)$ was obtained by two methods, the direct and the indirect (or perturbation) method. In the first method the Pierce expression for the interaction impedance must be used as a post processing calculation

$$K_0 = \frac{E_z(\rho=0)^2}{2\beta^2 P_T}, \quad (4)$$

where $E_z(\rho=0)$ is the axial electric field on axis and P_T is the total power propagated by the SWS. P_T is obtained setting the post processing routine to calculate the Poynting vector and integrate over a cross section of the structure. However, this method is not the most accurate for predicting the interaction impedance since an eigensolver is not capable of determining the summation of power propagated by all modes due to the normalization scheme intrinsically employed in the method. Some works have reported the use of the perturbation technique, mainly used in measurement methods, in the computational simulations of SWSs [2] [3]. In this method, the interaction impedance is assumed to be proportional to a deviation in the propagation constant $\Delta\beta/\beta$ when a little perturbation occurs on the field pattern [4]. A perturbation expression for the interaction impedance is given in [5] and used here is

$$K_0 = \frac{\Delta\beta}{\beta} \frac{Z_0}{\pi k_0 \beta (\varepsilon_p - 1)} \frac{1}{\tau}, \quad (5)$$

where Z_0 is the free space impedance and

$$\tau = \int_0^{r_p} I_0(\gamma\rho) I_0(\tilde{\gamma}\rho) \rho d\rho + \frac{\beta\tilde{\beta}}{\gamma\tilde{\gamma}} \int_0^{r_p} I_0'(\gamma\rho) I_0'(\tilde{\gamma}\rho) \rho d\rho. \quad (6)$$

In expression (6) $I_0()$ and $I_0'()$ are the modified Bessel function of the first kind and its first derivative, respectively. Perturbed quantities carry a tilde ($\tilde{\cdot}$). r_p and ε_p are the radius and the relative electric permittivity, respectively, of a dielectric rod inserted in the axis of the slow-wave structure to create the perturbed field pattern. The choice of a good perturber rod, i.e. r_p and ε_p , is an important task, since the perturbation must be small in order to not change significantly the electromagnetic behavior of the device under test, but must also be sufficiently large to be measurable with good precision. Figure 5 presents the deviation on the unperturbed eigenfrequency due to the insertion of a perturber rod with variable radius and relative permittivity. The perturbation in the eigenfrequency is nearly a quadratic function of the perturber parameters. Therefore, for a hypothetical perturber with radius of $0.1 a_i$, a large variation in the electric permittivity

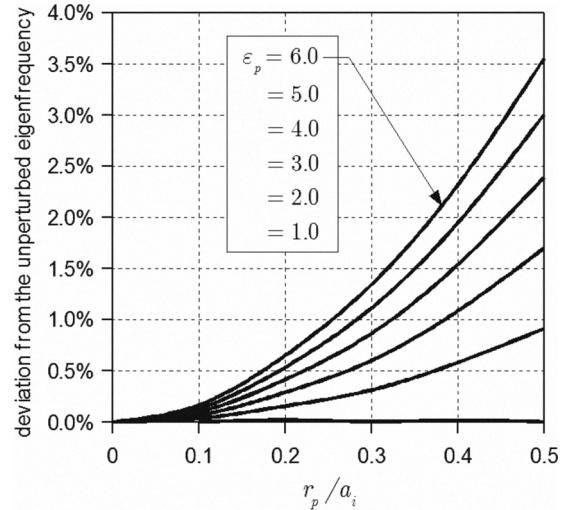


Figure 5 – Deviation in the unperturbed eigenfrequency due to the insertion of a perturber rod with variable radius and relative permittivity. a_i is the inner radius of the ring-bar slow-wave structure.

will not result in a large variation in the measured interaction impedance. However, this level of perturbation might not be measurable with good precision.

C. Simulation with the frequency domain solver

Using the frequency domain solver turns the simulation very similar to the measurement procedure discussed in the next section. The objective is to obtain the axial electric field phase (in radians) as a function of the axial position $\Phi(z)$. From this result, the propagation constant β may be found using [6]

$$\beta = \frac{1}{2} \frac{d\Phi(z)}{dz}. \quad (7)$$

An alternative way is to find the guided half-wavelength ($\lambda_g/2$) measuring the distance between two points of same phase in the $\Phi(z)$ data. The propagation constant is given by

$$\beta = \frac{2\pi}{\lambda_g}. \quad (8)$$

In this case, special care has to be taken in order to not use the ends of the $\Phi(z)$ data, which are distorted due to the non periodic behavior of the electromagnetic fields in these regions. Taking an average of the values of $\lambda_g/2$ in the middle region of the structure is a good practice. The interaction impedance can be obtained, in this case, only by a perturbation method using (5)-(6). The deviation in the propagation constant is obtained by using one of the methods just discussed (7)-(8) in the perturbed and unperturbed case.

Compared to the eigenmode solver, the frequency domain solver has a disadvantage related to the number of periodic cells necessary to simulate the SWS. The guided wavelength is increased in the lower frequencies, making necessary to increase the number of periodic cells and, therefore, the

number of mesh cells and computational time. Additionally, the obtaining of the propagation constant by the half-wavelength may be quite laborious when compare to the eigensolver method. However, the frequency domain solver may be very elucidative when planning a measure experiment.

D. Measurements

The phase velocity measurement procedure [5] consists in to obtain the curve $\Phi(z)$ by measuring the phase of the S_{11} or S_{22} scattering parameter of the slow-wave structure while a helical short-circuit is displaced along the structure axis. From this curve, (7) and/or (8) may be applied to obtain the propagation constant and, therefore, the phase velocity. A helical short-circuit of 3 turns and radius $a_i/2$ was used because of its broadband characteristics [6]. This short-circuit is supported by a small Lucite rod guided by a thin nylon wire. Figure 6 presents a comparison among experimental results using (7) and (8) and the simulation of the eigenmode solver. No appreciable discrepancy between both measurement results was noted. The simulated result differs in about 4% over the whole frequency band. This discrepancy was thought to be due to a systematic error introduced by the helical short circuit displacement system, which loads the slow-wave structure with electric permittivity due to the nylon and the Lucite. However, this effect could not be experimentally quantified.

The experimental interaction impedance was obtained using (5)-(6). The deviation in the propagation constant was obtained measuring the phase of the S_{11} scattering parameter in the absence of perturbation and in the presence of a PVC perturber rod of radius $a_i/3$ and relative permittivity around 3.0. The perturbation of a nylon wire of radius $a_i/7$ was poorly measurable and led to non conclusive results. Measurements with perturber elements with smaller radius or lower electric permittivity also led to non conclusive results. Figure 7 presents the comparison between simulated and experimental interaction impedances. Simulated interaction impedance using direct method presented discrepancy of 2 to

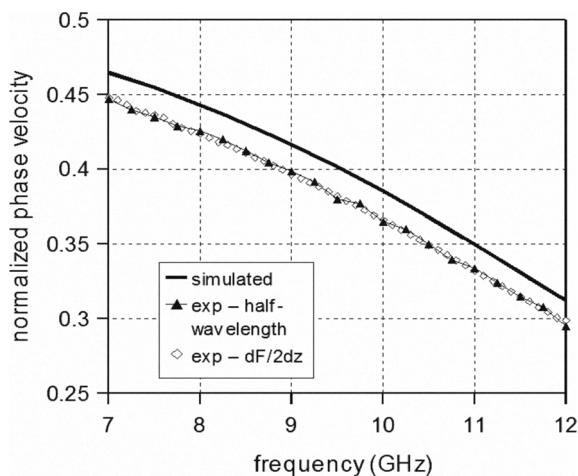


Figure 6 – Comparison among experimental and simulated results for the phase velocity of the slow-wave structure analyzed.

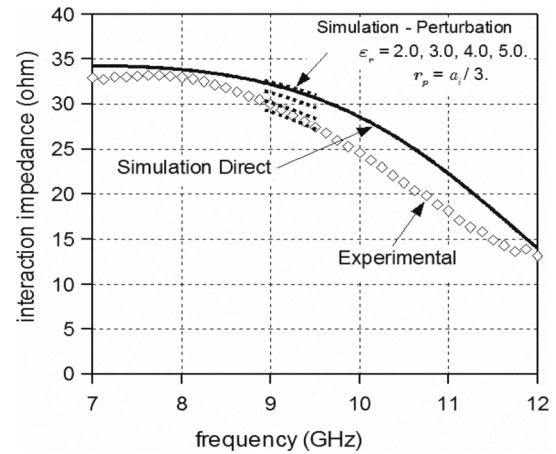


Figure 7 – Comparison among experimental and simulated results for the interaction impedance of the slow-wave structure analyzed.

8% in relation to the experimental one. The discrepancy observed between 9-12 GHz may be due to the frequency dependency of ϵ_p , which was ignored in the data analysis. Simulated curves for electric permittivity about 4 and 5 achieved better agreement.

IV. CONCLUSION

A review and improvements were made on the interaction circuit of an X-band traveling-wave tube using the CST Microwave Studio CAD tool. A ladder type impedance transformer was designed for a specified frequency range and suitably characterized. Additionally, the slow-wave structure of this interaction circuit was successfully modeled and characterized. The discrepancies between simulated and experimental results were computed and considered satisfactory.

REFERENCES

- [1] D. T. Lopes and C. C. Motta, "Dispersion and Impedance Determination on Slow-Wave Structures for High-Power Traveling-Wave Tubes," *IEEE Trans. Electron Devices*, vol. 5, No. 9, Sept. 2008.
- [2] Carol L. Kory and James A. Dayton, "Computational Investigation of Experimental Interaction Impedance Obtained by Perturbation for Helical Traveling-Wave Tube Structures," *IEEE Trans. Electron Devices*, vol. 45, pp. 2063–2071, Sept. 1998.
- [3] C. T. Chevalier, C. L. Kory, J. D. Wilson, E. G. Wintucky, and J. A. Dayton, Jr., "Traveling-wave tube cold-test circuit optimization using CST MICROWAVE STUDIO," *IEEE Trans. Electron Devices*, vol. 50, no. 10, pp. 2179–2180, Oct. 2003..
- [4] R. P. Lagerstrom, "Interaction impedance measurements by perturbation of traveling waves," Tech. Rep. no. 7, Stanford Electronics Laboratories, Stanford Univ., Stanford, CA, Feb. 11, 1957..
- [5] D. T. Lopes, "Caracterização de estruturas de ondas lentas helicoidais para utilização em TWT de potência", M.Sc. dissertation, Instituto de Pesquisas Energéticas e Nucleares, Universidade de São Paulo, São Paulo, 2007.
- [6] S. J. Rao, S. Ghosh, P. K. Jain, and B. N. Basu, "Nonresonant perturbation measurement on dispersion and interaction impedance characteristics of helical slow-wave structures," *IEEE Trans. Microwave Theory Tech*, vol. MTT-45, pp. 1585-1168, Sep. 1997